"THEORETICAL ANALYSIS OF DIRECTLY COUPLED 8-12 μm HYBRID IRCCD SERIAL SCANNING (U)"

A. J. Steckl
Honeywell
Radiation Center

Toivo Koehler
Honeywell
Radiation Center

ABSTRACT. The hybrid IRCCD consists of a linear array of infrared photodiodes directly coupled to a silicon CCD shift register. In the serially scanned mode, the detector outputs corresponding to the same resolution element are delayed-and-added. The direct coupling concept is first discussed. Then a general relation for the IRCCD output signal-to-noise ratio is developed. For a typical application consisting of an array of nine 12 μm (Hg,Cd)Te photodiodes receiving an incident flux of 3×10^{17} photons/cm^2-s (T_S = 300 °K, FOV = 90°), the following values were calculated: $S_O/N_O \cong 500$, $NE\Delta T \cong 0.1$ °K, Dynamic Range ≅ 300.

INTRODUCTION

The two main obstacles to the application of charge coupled devices and concepts to the area of thermal imaging are the high background flux and the low contrast ratio present at infrared wavelengths. The serially scanned TV-compatible Framing Infrared (FIR) system is one case where these problems are circumvented and where the coupling of IR detectors to a silicon CCD (the IRCCD) in a hybrid structure represents an appealing alternative to the present mode of operation.

The serially scanned FIR uses a linear array of detectors raster scanned across the scene, the scan direction being parallel to the array[1],[2]. Since each detector in turn scans the entire field of view, the dwell time per resolution element for the case analyzed in this paper is approximately 150 ns. The amount of charge generated during this dwell time in an 8-12 μm IR detector by a 300 °K blackbody is well within the charge handling capacity of a typical CCD shift register. By processing the outputs of the detectors through a delay-and-add operation, the components of the signals corresponding to the same resolution element are summed linearly. Because the noise contribution of each detector is independent and thus uncorrelated, the total noise is obtained by a root mean square summation. For an array of m detectors, the delay-and-add operation could therefore result in a maximum improvement of $\sqrt{m}$ (in the detector noise limited case) in the signal-to-noise ratio (SNR) of the entire array over that of an individual detector. The upper limit of m and therefore of the maximum SNR improvement achievable is set by the total detector array signal versus the CCD charge capacity. The operation of the entire array appears at the CCD output essentially as one detector. This results in no fixed pattern noise, lowered detector response

uniformity requirements as well as built-in redundancy. These features together with the potential $\sqrt{m}$ improvement in SNR should help circumvent the problems posed by the high background and low contrast ratio present in thermal imaging systems at infrared wavelengths.

HYBRID IRCCD OPERATION

DIRECT COUPLING CONCEPT

At the heart of the hybrid IRCCD imaging device is the technique of direct coupling (i.e. without a buffer stage) between an IR photovoltaic detector and the silicon CCD analog shift register. This technique can be accomplished by several methods which are closely related to the input schemes proposed for and employed in other applications of CCD and 'Bucket Brigade' analog shift register[3],[4]. One possible mode of operation being investigated is shown in Figure 1 for n-on-p IR photodiodes and an n-channel CCD. The IR photodiodes are each connected in parallel to a silicon coupling diode (SCD) diffused into the same silicon substrate on which the CCD is fabricated. The first MOS gate (ENTER) of the CCD would then perform two functions: (a) to reverse bias the IR diode and the silicon coupling diode, (b) to allow the introduction of photocharge into the CCD through a field induced n-channel. When the $\phi 1$ gate is activated with a positive pulse, the potential well under the gate acts as a sink for the diodes and the photocurrent plus the saturation currents of the diodes will flow into the well for the duration of the $\phi 1$ pulse. When the $\phi 2$ gate is turned on and the $\phi 1$ gate is turned off the current flow stops and the charge present is transferred on through the device.

DEVICE ORGANIZATION

A typical IRCCD array organization is shown schematically in Figure 2. The CCD shift register shown is three phase (though the two- or four-phase type would apply equally well) with an input (source) diffusion, an output diffusion, and a reset output diffusion. The purpose of the input diffusion is twofold: (a) to allow the characterization of the CCD independent of the IR photodiode array, (b) to allow for the circulation of a constant amount of charge in the CCD ("fat" zero) and thus reduce the transfer inefficiency. The output diffusion, which collects the charge from the last CCD bit, is connected to the gate of a MOS transistor. Once during each clock cycle, the output diffusion is reset by energizing the reset transfer gate and thus returning the output diffusion to its initial potential. In addition, there are diffusions (adjacent to the $\phi 1$ electrode of each CCD bit) making up the SCD array. The SCD array is separated from the CCD by the MOS enter gate running the length of the shift register. Finally, there is an IR photodiode connected in parallel to each SCD.

DELAY-AND-ADD OPERATION

The operation of the IRCCD imaging device is detailed below. The signal charge which is transferred into each bit of the CCD corresponds to the incident radiation in the respective resolution element of the scene being viewed by each detector. The clocking frequency of the CCD is synchronized with the mechanical scanner such that the input from detector 1 corresponding to a given resolution element is shifted from the first to

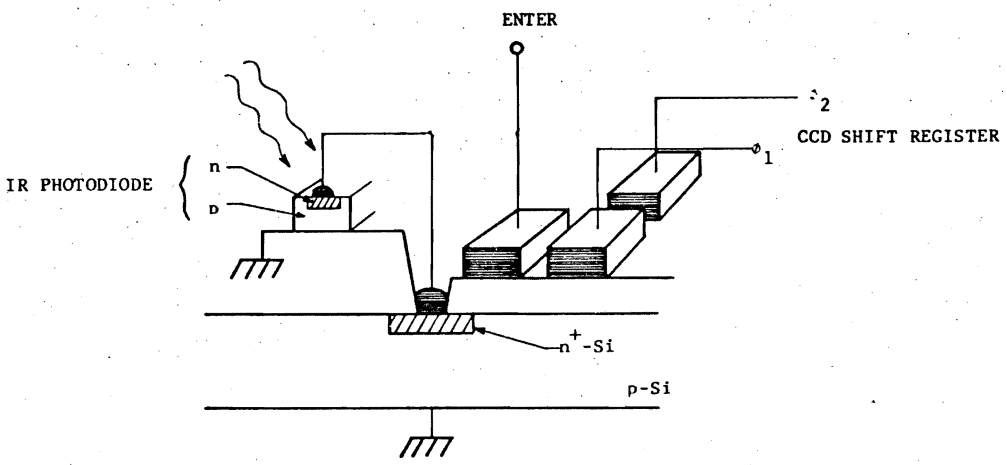

Figure 1 IRCCD CONFIGURATION (HATCHED AREAS REPRESENT DIFFUSIONS): DIRECT COUPLING CONCEPT

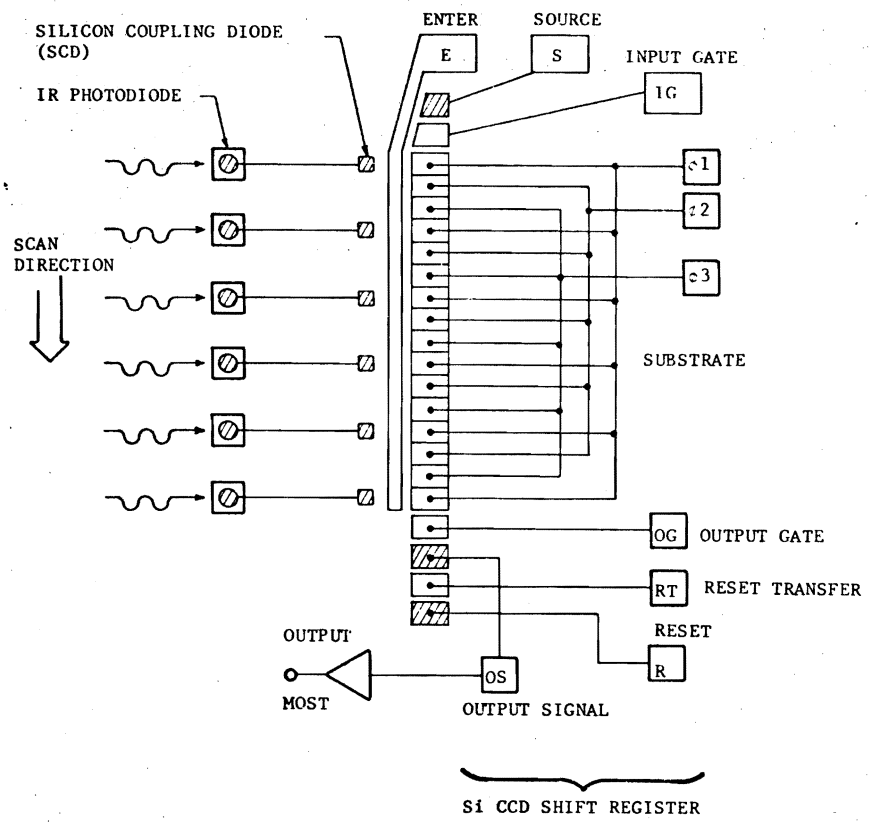

Figure 2 IRCD ORGANIZATION

the second bit of the CCD such that it is added to the input from detector 2 corresponding to the same resolution element one dwell time later. The same process applies sequentially to all the inputs to the CCD. In this manner each output charge packet of the CCD contains the summation of all inputs (both signal and noise) corresponding to the same resolution element of the scene. This particular application of the CCD can thus be characterized as a parallel-to-series converter operated in the delay-and-add mode.

ANALYSIS

Most of the figures of merit of any electronic device are derived from its signal-to-noise ratio (SNR). Since this is especially true for a thermal imaging device, the general SNR relation for the serially scanned directly coupled hybrid IRCCD (described above) is first developed. Next the various noise contributions of the IRCCD are given. It is important to note here that in this first analysis certain assumptions introduced below are used both because they seem reasonable and for the sake of simplicity. However, it is felt that once the analytical framework is set up it can be further refined and modified by the relaxation of initial assumptions and the introduction of previously neglected noise sources. Finally, the formalism is applied to the case of a TV-compatible 8-12 μm FIR and several important operational parameters are calculated.

SIGNAL-TO-NOISE RATIO: GENERAL RELATION

The noise contributions of the IRCCD can be naturally classified according to their origin in one of the three stages of the device: (a) the detector array, (b) the SCD/CCD array, and (c) the output MOST/transistor stage. Within each stage there are a number of noise sources which are discussed in greater detail below. In addition, the last two stages have an associated gain factor which is smaller than one in the SCD/CCD array (due to charge transfer inefficiency) and larger than one in the output preamplifier stage. Charge coupled devices are naturally analyzed in terms of the charge or the number of carriers in a packet and the procedure lends itself very well to the analysis of the IRCCD. The signal, therefore, corresponds to the number of photogenerated carriers transferred into the CCD during one read time, t_R. The noise sources are translated into rms fluctuations in the total number of carriers in each charge packet. Figure 3 is a schematic which indicates the terminology associated with each stage of the device as outlined in Table I below.

TABLE I NOTATION

R_i	i^{th} Detector	Current Responsivity
S_i		Signal
N_i		Noise
N_A	CSD/CCD Array	Noise at CCD Output
A		Attenuation/Bit
N_G	Output Preamp Stage	Noise at Preamp Input
G		Gain
S_o	Output	Signal
N_o		Noise
W	Incident Radiation Power (watts)	

The detector noise has two components:

$$\bar{N}_i^2 = \bar{N}_{ip}^2 + \bar{N}_{iq}^2 \qquad (1)$$

The $\bar{N}_{ip}$ component is a function of detector current and therefore will be affected by the number of carriers in the charge packet, while the $\bar{N}_{iq}$ component is independent of the detector current. In the delay-and-add

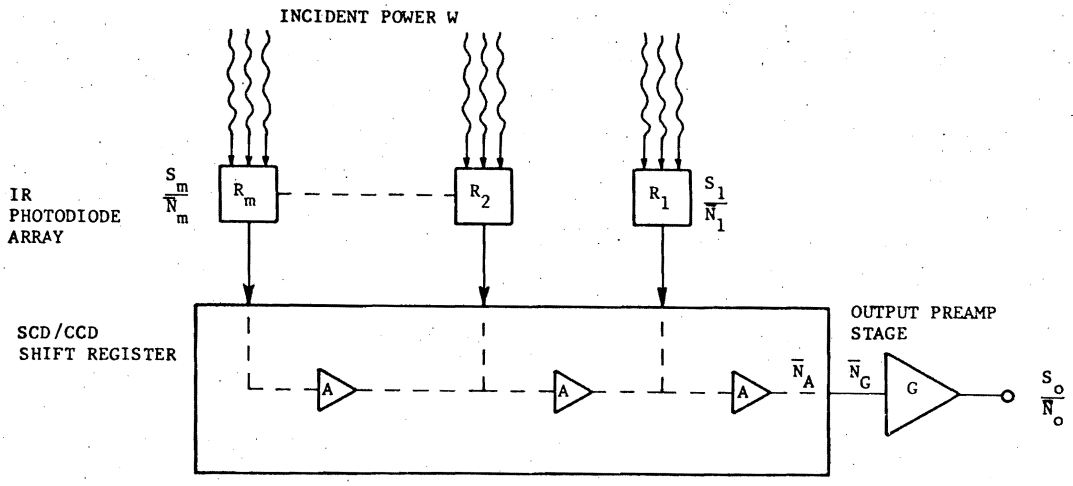

Figure 3 IRCCD SCHEMATIC, SHOWING TERMINOLOGY ASSOCIATED WITH SIGNAL-TO-NOISE ANALYSIS

mode, the IRCCD output signal corresponding to one resolution element of the scene consists of the sequential summation of all the individual detector outputs generated when radiation from the resolution element was scanned across the array. For a resolution element which is radiating signal power in the amount W_s, the output peak signal and the rms noise of an IRCCD sensor having m detector channels and an m bit (with p gates/bit) SCD/CCD shift register is given by:

$$S_o = W_s G\left\{R_1 A + R_2 A^2 + \ldots + R_m A^m\right\}\frac{t_R}{q} \quad (2)$$

$$= W_s G \frac{t_R}{q} \sum_{i=1}^{m} R_i A^i \quad (3)$$

$$\bar{N}_o = G\left\{\bar{N}_{1p}^2 A^2 + \ldots + \bar{N}_{mp}^2 A^{2m} + \right.$$

$$\left. + \bar{N}_{1q}^2 + \ldots + \bar{N}_{mq}^2 + \bar{N}_A^2 + \bar{N}_G^2\right\}^{\frac{1}{2}} \quad (4)$$

$$= G\left\{\sum_{i=1}^{m}\left[\bar{N}_{ip}^2 A^{2i} + \bar{N}_{iq}^2\right] + \right.$$

$$\left. + \bar{N}_A^2 + \bar{N}_G^2\right\}^{\frac{1}{2}} \quad (5)$$

where q is the electronic charge and t_R is the read time. The output signal-to-noise ratio then has the following general form:

$$\frac{S_o}{\bar{N}_o} = \frac{t_R W_s \sum_{i=1}^{m} R_i A^i}{q\left\{\sum_{i=1}^{m}\left[\bar{N}_{ip}^2 A^{2i} + \bar{N}_{iq}^2\right] + \bar{N}_A^2 + \bar{N}_G^2\right\}^{1/2}} \quad (6)$$

If a high overall transfer efficiency exists,

$$m(1 - A) \leq 0.1$$

the individual signal and noise from each detector can be replaced in equation 6 by the average value over the array, $R_i=R$, $\bar{N}_{ip}=\bar{N}_p$, $\bar{N}_{iq}=\bar{N}_q$

$$\frac{S_o}{\bar{N}_o} = \frac{m t_R W_s R}{q\left[m(\bar{N}_p^2 + \bar{N}_q^2)+\bar{N}_A^2+\bar{N}_G^2\right]^{\frac{1}{2}}} \qquad (7)$$

In the case where the IRCCD is detector noise limited, equation 7 is approximated by:

$$\frac{S_o}{\bar{N}_o} \cong \frac{\sqrt{m}\ t_R W_s R}{q(\bar{N}_p^2 + \bar{N}_q^2)^{\frac{1}{2}}} = \sqrt{m}\ \frac{S}{\bar{N}} \qquad (8)$$

where $S/\bar{N}$ is the signal-to-noise ratio of an individual detector. Equation 8 shows the maximum $\sqrt{m}$ improvement in SNR characteristic of the delay-and-add operation.

IRCCD NOISE SOURCES

In the first stage of the IRCCD, the photodiode array, the noise sources are those associated with photovoltaic detectors operating in the reverse bias mode[5][6]:

a. Shot noise generated by the total current flow, reverse bias dark current I(V) and photocurrent Ip:

$$\bar{i}^2_{N,Sh} = 2q\left[I_p + I_o(e^{qV/kT_D}+1)\right]\Delta f \qquad (9)$$

where T_D is the detector temperature and Δf is the measuring bandwidth.

b. Nyquist (Johnson) noise due to the shunt conductance G_S of the diode is:

$$\bar{i}^2_{N,J} = 4kT_D\ G_S\ \Delta f \qquad (10)$$

Associated mainly with the shunt conductance there is a 1/f noise component which can, however, be eliminated with proper filtering. For a reverse bias resulting in a potential larger than a few kT_D, the photodiode noise current can be rewritten as

$$\bar{i}^2_N = 2\Big\{\left[qI_p + kT_D G_J(o)\right] + \left[2kT_D\right]\Big\}\ \Delta f \qquad (11)$$

where $G_J(o)$ is the zero bias junction conductance. The photocurrent is the result of radiation incident on the detector and it has two components: background photocurrent (due to radiation from housing, optics, and filters) and signal photocurrent (due to radiation from the scene):

$$I_p = RW = q\eta A_D\ (\Phi_s + \Phi_B) \qquad (12)$$

where A_D is the detector area, Φ_S and Φ_B are the signal and background photon fluxes. The direct coupling efficiency, η, is defined as the relative percentage of carriers introduced into the $\phi 1$ potential well of the CCD per unit number of incident photons. The number of carriers in the charge packet corresponding to the i^{th} detector signal and background is then obtained by integrating the signal current over the read time,

$$S_i = W_s R_i \frac{t_R}{q} = A_D t_R\ \Phi_s \eta_i \qquad (13a)$$

$$N_{B,i} = W_B R_i \frac{t_R}{q} = A_D t_R\ \Phi_B \eta_i \qquad (13b)$$

Translating the detector noise current into rms fluctuations in the

number of carriers in the packet, the noise of the i^{th} detector is then given by:

$$\overline{N}_i^2 = \overline{N}_{ip}^2 + \overline{N}_{iq}^2$$

$$= \frac{t_R}{q^2}\left\{\left[q^2\eta_i A_D(\Phi_s+\Phi_B)+ kT_D G_J(o)\right]\right.$$

$$\left. + [2kT_D G_S]\right\} \qquad (14)$$

The current dependent and independent terms $\overline{N}_{ip}$ and $\overline{N}_{iq}$ respectively, of the detector noise are given by the first and second sets of brackets on the RHS of equation 14.

In the second stage of the IRCCD, the SCD/CCD array, the following main noise sources are present(7)(8)(9):

a. Shot noise and Nyquist noise of the silicon coupling diode is negligible and will not be introduced in the analysis.

b. Reset noise associated with the introduction of "fat" zero charge through the CCD input diffusion into the first potential once during each clock cycle:

$$\overline{N}_{A,FZ}^2 = \frac{kT_o C_{FZ}}{q\,2} \qquad (15)$$

where C_{FZ} is the capacitance of the CCD input diffusion.

c. Fluctuations in the charge packet due to transfer loss are given by

$$\overline{N}_{A,T}^2 = 2(1-A)\left\{[(S_1+N_{B,1})A + \ldots\right.$$

$$\left. + (S_m+N_{B,m})A^m]+ N_{CCD,F2}\right\} \qquad (16a)$$

$$= 2(1-A)\sum_{i=1}^{m}(S_i+N_{B,i})A^i \qquad (16b)$$

where S_i plus $N_{B,i}$ represent the total number of carriers in the charge packet introduced by the i^{th} detector and $N_{CCD,F2}$ is the number of fat zero carriers introduced into the CCD. The transfer efficiency A was assumed to be independent of the amount of charge being transferred(7). Assuming an average charge packet, a high transfer efficiency and a relatively small number of bits, the transfer loss fluctuation noise term is given by the simplified realtion: (16)

$$\overline{N}_{A,T}^2 = 2m\,(1-A)\left[(S + N_B)+N_{CCD,F2}\right]$$

d. Carrier fluctuations due to carrier generation and recombination in fast interface states are given by

$$\overline{N}_{A,SS}^2 = 1.4\ kT_o n_{SS}\ mpA_g \qquad (17)$$

for the "fat" zero mode of operation. n_{SS} is the density of interface states and A is the CCD area/gate.

In the output amplifier stage of the IRCCD, the main noise sources are(8):

a. Thermal noise of the reset channel of the output diffusion,

$$\overline{N}_{G,o}^2 = \frac{kT_o C_o}{q^2} \qquad (18)$$

where C_o is the combined capacitance of the output and reset diffusions and the MOST input capacitance.

b. Input noise of the MOST due to thermal fluctuations in the source to drain channel conductance:

$$\overline{N}_{G,MOST}^2 = \frac{C_g^2}{q^2}\ \frac{4kT_o}{g_m}\ \Delta f \qquad (19)$$

where g_m is the MOST transconductance, C_g is the MOST gate capacitance. The 1/f noise component is assumed to be eliminated by the proper filtering technique.

CALCULATIONS

In performing calculations for the signal-to-noise ratio and related figures of merit, typical rather than best-case values obtained either at

Honeywell or elsewhere were chosen for the parameters and characteristics of each of the three stages of the IRCCD.

For the detector array, $Hg_{0.8}Cd_{0.2}Te$ photodiodes were considered[11]. These devices are routinely fabricated at Honeywell on p-type (Hg,Cd)Te substrate. The junction and n-layer are formed by either indium ion implantation or mercury diffusion and the active area is defined by a mesa etch. These devices have achieved quantum efficiencies of 50% (without antireflection coating), R_JA products of 0.3 ohm-cm^2, and shunt resistances of 1.6 kohms at 77 °K.

The feasibility of fabrication and operation of a silicon CCD as a parallel-to-series converter (similar to the shift register described above) has been shown at Honeywell with a three phase device[12].

The parameters and calculated noise contributions of a typical IRCCD operating in a serially scanned FIR system are given in detail in Table II. Some of the salient features are discussed here:

a. For the conditions of operation chosen (Φ_S, A_D, t_R, etc.) the number of photogenerated carriers per detector is 6×10^5. The maximum number of carriers which can be handled by the CCD is 1.7×10^7 for a gate area of 20 μm x 40 μm, oxide thickness of 1000 Å and effective gate voltage of 10 V. Under these conditions, the output of up to 25 detectors can be summed by the CCD before saturation is reached, assuming that a fat zero amounting to 10% of the maximum capacity is being circulated.

b. For the transfer efficiency/bit of 0.9997 and a CCD of nine bits, the overall efficiency is 0.997, more than sufficient justification for replacing the individual detector signal and noise with the average value over the array (see equations 6 and 7).

c. The dominant noise mechanism in the detector array is the Johnson noise of the shunt conductance. It is expected that with improved surface passivation techniques the shunt conductance will be significantly lowered. The dominant noise mechanism in the SCD/CCD array is due to surface state g-r current. This component can also be reduced through surface passivation or avoided by using a buried channel CCD. Overall, the detector noise component is the largest component in the IRCCD.

d. The dynamic range of an IRCCD with m detector channels can be defined as the ratio of $1/m^{th}$ maximum usable carrier capacity of an individual potential well to the minimum detectable number of carriers:

$$D.R.= \frac{N_{CCD,MAX}-(mN_B+N_{CCD,FZ})}{m\left[m(\bar{N}_q^2+\bar{N}_p^2)+\bar{N}_A^2+\bar{N}_G^2\right]^{\frac{1}{2}}} \qquad (20)$$

$N_{CCD,MAX}$ is the number of carriers required to fill up the potential well; N_B and $N_{CCD,FZ}$ are the number of background carriers introduced optically and electrically. Using the parameters given in Table II, the IRCCD dynamic range is plotted as a function of the number of detectors and for three values of fat zero in Figure 4.

e. The output signal-to-noise ratio for this example has been calculated to be approximately 490. The improvement due to the delay-and-add operation of the nine detectors in the array is about 2.99 which is 99.7% of the maximum possible improvement of 3.

TABLE II PARAMETERS AND CALCULATED NOISE CONTRIBUTIONS OF TYPICAL IRCCD OPERATING IN SERIALLY SCANNED FLIR SYSTEM

	PARAMETERS			NOISE CONTRIBUTIONS		
	SYMBOL	DEFINITION	VALUE	SYMBOL	DEFINITION	VALUE
Incident Radiation	FOV	Field of View	90°			
	T_B	Background Temperature	80 °K	$\frac{S_o}{N_o}$	IRCCD Output Signal-to-Noise Ratio	490
	T_S	Scene Temperature	300 °K			
	Φ_S	Photon Flux (Scene)	3×10^{17} cm^{-2}-s^{-1}			
	Φ_B	Photon Flux (Background)	6.3×10^{13} cm^{-2}-s^{-1}			
Detector Array	A_D	Detector Area	2×10^{-5} cm^2			
	C_J	Junction Capac.	1×10^{-12} F	$\bar{N}_p$	Shot Noise	767
	G_J (0)	Zero Bias Junc. Cond.	6.7×10^{-5} mho			
	G_J (V)	Reverse Bias Junc. Cond.	Negligible			
	G_S	Shunt Conductance	3.3×10^{-4} mho			
	m	No. of Detectors	9			
	N_B	No. of Background Carriers	63	$\bar{N}_q$	Johnson Noise	1690
	S	No. of Signal Carriers	6×10^5			
	T_D	Detector Temperature	80 °K			
	V_R	Reverse Bias	2 V			
	η	Coupling Eff.	0.5			
	λ_{co}	Cut-Off Wavelength	12 μm	$\bar{\Sigma}$	rms Summation	1415
	$\Delta\lambda$	Spectral Region	8-12 μm			
SCD/CCD Array	A	Transfer Eff/Bit	0.9997			
	Ag	Gate Area	8×10^{-6} cm^2			
	C_I	Total Input Cap	1×10^{-12} F	$\bar{N}_{A,FZ}$	Input Reset Noise	126
	C_{FZ}	CCD Input Cap	1×10^{-13} F			
	C_o	Total Output Cap	5×10^{-13} F			
	f_c	Clocking Frequency	6.5×10^6 Hz	$\bar{N}_{A,T}$	Transfer Loss	111
	n_{ss}	Interface State Density	1×10^{10} (cm^2-eV)$^{-1}$			
	$N_{CCD,FZ}$	No.of Fat Zero Carriers	1.7×10^6			
	$N_{CCD,max}$	Max No. of Carriers	1.7×10^7	$\bar{N}_{A,SS}$	Surface State Noise	280
	p	No. of Gates/Bit	3			
	T_o	CCD Temperature	300 °K			
	t_R	Read Time	1×10^{-7} s	$\bar{\Sigma}$	rms Summation	325
	V_G	Gate Voltage	12 V			
	V_T	Threshold Voltage	2 V			
Output Preamp	g_m	Most X Conductance	10^{-3} mho	$\bar{N}_G$	Output Reset Noise	285
	Δf	Bandwidth	3×10^6 Hz	$N_{G,Most}$	Most Channel Noise	8.8
	C_g	Most Gate Capacitance	2×10^{-13} F	$\bar{\Sigma}$	rms Summation	285

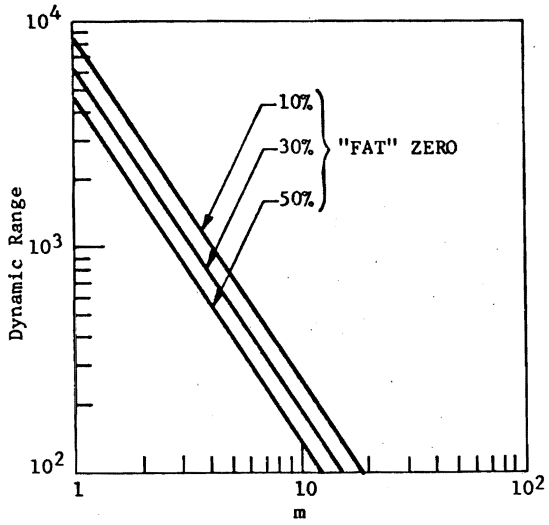

Figure 4 IRCCD DYNAMIC RANGE VS NUMBER OF DETECTORS

The output signal-to-noise ratio was also calculated over a broad range of incident signal flux, as shown in Figure 5. The variation in signal flux in the same 8-12 μm wavelength region can be the result of either the variation of the field of view (only up to FOV=2π, Φ_S=6x10^{17} photons/cm^2-s) or of different scene temperatures. A maximum value of S/N=3500 is reached at the maximum charge handling limit of the two detector CCD. This limit is reached at a flux of 8x10^{18} photons/cm^2-s. For an array of 25 detectors the maximum value of S/N=1600 is reached at a flux of approximately 6x10^{17} photons/cm^2-s.

In order to relate the IRCCD signal-to-noise ratio to its thermal sensitivity the figure of merit noise equivalent change in temperature is introduced (NEΔT). The NEΔT of the system is the change in scene temperature which generates a change in the number of output signal carriers equal to the number of output noise carriers:

$$\bar{N}_o = \frac{dS_o}{dT} \text{ NE}\Delta T \qquad (21)$$

Defining $\Delta\Phi_S(T_S,1\ ^\circ K)$ as the change in signal photon flux due to a 1 °K change in the temperature T_S of the scene, NEΔT can be related to the signal-to-noise ratio:

$$\text{NE}\Delta T = \frac{\Phi_S(T_S)/\Delta\Phi_S(T_S,1\ ^\circ K)}{S_o/\bar{N}_o} \qquad (22)$$

For the example given in Table II (T_S = 300 °K, FOV = 90°) the signal-to-noise ratio of 490 corresponds to a NEΔT $\simeq$ 0.12 °K. Two sets of constant NEΔT lines are superimposed on the SNR plot of Figure 5:

a. The first set is at the constant scene temperature of 300 °K. It can be seen, for example, that to achieve at this scene temperature a NEΔT = 0.1 °K requires a flux of almost 8x 10^{17} for a two detector array while only a flux of 2x10^{17} is required for an array of 25 elements.

b. The second is at a constant FOV (180°) but at the respective scene temperature indicated by the lower scale in Figure 5. To achieve the same NEΔT = 0.1 °K but with an FOV = 180 degrees requires a scene temperature T_S = 340 °K with a corresponding photon flux of 1x10^{18} for a two element array, but can also be achieved at a scene temperature T_S = 210 °K with a photon flux of 1.5x10^{17} with an array of 25 elements.

Finally, the improvement in both $S_o/\bar{N}_o$ and NEΔT as a function of the number of detectors in the array is plotted in Figure 6 for a constant scene temperature T_S = 300 °K and two values of FOV = 50 degrees, 90 degrees. A fourfold increase in detectors from an array with four elements to one with sixteen elements, results in a lowering of the NEΔT by about a factor of two for both fields of view. However, increasingly smaller returns are gained by increasing the number of detectors past a certain level.

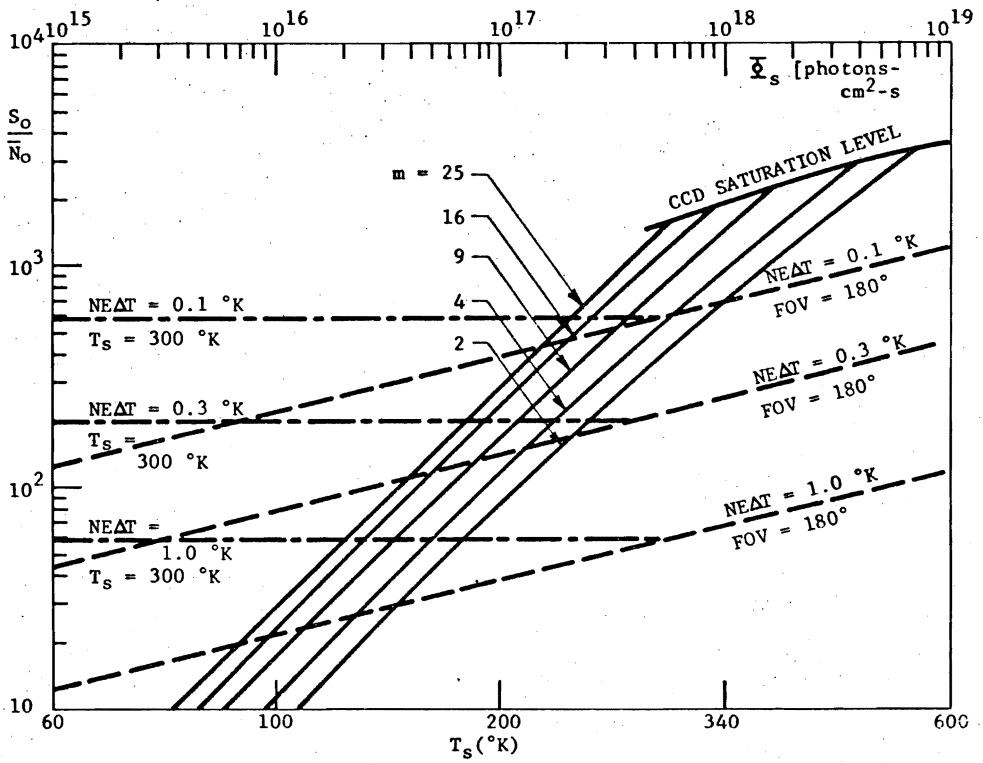

Figure 5 IRCCD SIGNAL-TO-NOISE RATIO AS A FUNCTION OF SIGNAL FLUX (OR SCENE TEMPERATURE) AND NUMBER OF DETECTORS IN ARRAY

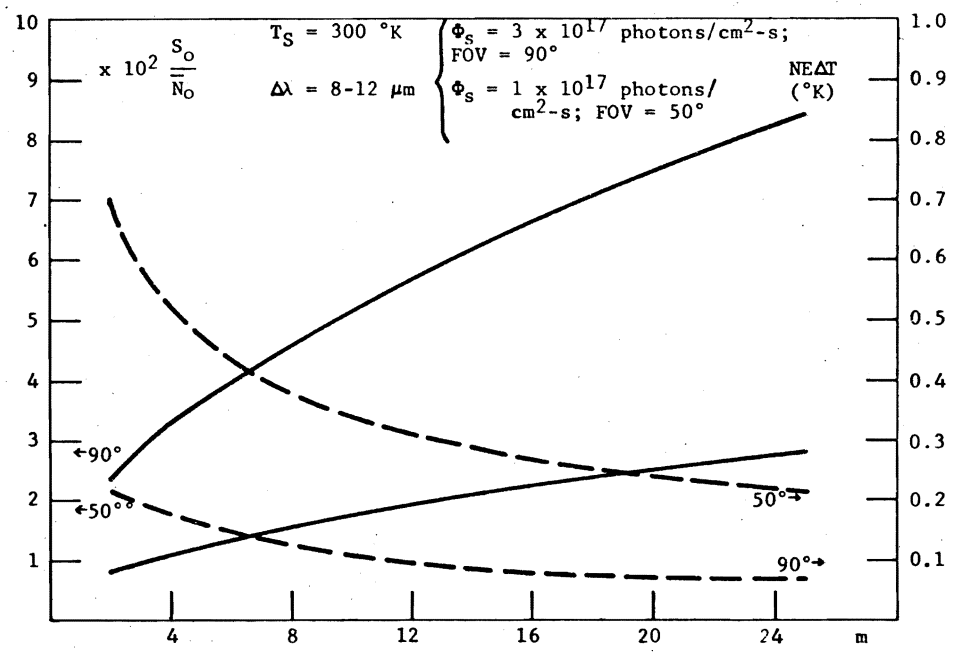

Figure 6 NOISE EQUIVALENT TEMPERATURE CHANGE AND SIGNAL-TO-NOISE RATIO VS NUMBER OF DETECTORS IN IRCCD ARRAY

SUMMARY AND CONCLUSIONS

The basic concept of the direct coupling IR photodiode/Si (SCD/CCD) has been described. On that basis the operation of the hybrid IRCCD serially scanned thermal imager has been discussed and analyzed. The general signal-to-noise ratio formalism for an n-channel, m detector IRCCD was developed. A typical example, m=9, was analyzed in detail resulting in the following calculated values: $S_o/\bar{N}_o \cong 500$, D.R.=300, $NE\Delta T \cong 0.1$ °K. These results indicate that the hybrid 8-12 μm directly coupled IRCCD is potentially a very useful thermal imaging device.

BIBLIOGRAPHY

(1) N.B. Stetson, J.M. Lloyd, and R.F. Anderson, The TV-FLIR Concept, 20th National IRIS Conf., June 1973, Monterrey, CA.

(2) A. Fenner Milton, Infrared Detectors for Serial Scanning, IRIS Detector Specialty Conf., March 1973, Washington, D.C.

(3) M.F. Tomsett and E.J. Zimany, Use of Charge Coupled Devices for Delaying Analog Signals, IEEE J. of Solid State Circuits, 8, 152 (1973).

(4) W.J. Butler, M.B. Barron, and C.M. Puckette, Practical Considerations for Analog Operation of Bucket Brigade Circuits, IEEE J. of Solid State Circuits, 8, 157 (1973).

(5) A. van der Ziel, Theory of Shot Noise in Junction Diodes and Junction Transistors, Proc. of IRE, p. 1641, Nov. 1955.

(6) G.R. Purett and R.L. Petritz, Detectivity and Preamplifier Considerations for InSb Photovoltaic Detectors, Proc. of IRE, 47, 1525 (1959).

(7) J.E. Carnes and W.F. Kosonocky, Noise Sources in Charge Coupled Devices, RCA Review, 33, 327 (1972).

(8) G.F. Amelio, W.J. Bertram, and M.F. Tomsett, Charge Coupled Imaging Devices: Design Considerations, IEEE Trans. on Electron Devices, 18, 986 (1971).

(9) D.F. Barbe, The Charge Coupled Concept, Report of NRL Progress, March 1972.

(10) F.M. Klaassen and J. Prins, Thermal Noise of MOS Transistors, Phillips Res. Reports, 22, 505 (1967).

(11) T. Koehler and D. Soderman, Mercury Cadmium Telluride 10.6-Micron Photodiode, Research and Development Technical Report, ECOM-0236-2, Submitted to U.S. Army Electronics Command under Contract DAAB07-71-C-0236, March 1973.

(12) W.E. Tchon and J.S.T. Huang, Personal Communication.